

SYNTHESIS AND CHARACTERIZATION OF POLY(ACRYLIC ACID-CO-ACRYLAMIDE)-SAWDUST COMPOSITE FOR THE ADSORPTIVE REMOVAL OF Cd(II) AND Pb(II) FROM AQUEOUS SOLUTIONS

Abdul Qayyum KHAN,^a Ata Ur RAHMAN,^{a*} Muhammad YASEEN,^a Haroon Ur RASHID,^b
Mahmood IQBAL^c and Mushtaq Ur REHMAN^c

^aInstitute of Chemical Sciences, University of Peshawar, 25120, Peshawar, KP, Pakistan

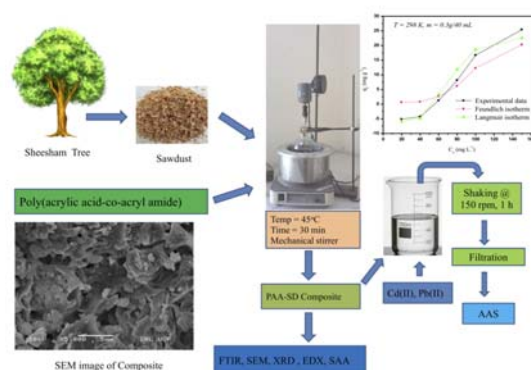
^bDepartment of chemistry, Sarhad University of Science and Information Technology, Peshawar, KP, Pakistan

^cPakistan Council for Scientific and Industrial Research (PCSIR) Laboratories Complex, University Road Peshawar, KP, Pakistan

Received December 27, 2017

A novel poly(acrylic acid-co-acrylamide)/sawdust composite was synthesized by copolymerization of partially neutralized acrylic acid and acrylamide with sawdust using N,N-methylenebisacrylamide as a crosslinker and potassium persulfate/sodium sulphite as initiators. The composite was characterized by FTIR, XRD, SEM, EDX and BET techniques. The adsorption of Cd(II) and Pb(II) ions on composite in aqueous solution was studied in batch experiments optimizing reaction parameters like initial concentration, contact time, pH and temperature. The adsorption kinetics followed pseudo second order kinetic model. Adsorption isotherms were applied to the experimental data which fitted well with Langmuir and Freundlich isotherms. The maximum adsorption capacities (q_m) (from Langmuir model) of the prepared composite at 25 °C, were 28.57 mg g⁻¹ and 32.25 mg g⁻¹ for Cd(II) and Pb(II) ions, respectively. Activation energy data (12.148 kJ mol⁻¹ and 7.165 kJ mol⁻¹ Cd(II) and Pb(II), respectively) indicated physisorption. Results of thermodynamic parameters like ΔG° , ΔH° and ΔS° for both Cd(II) and Pb(II) ions suggested the spontaneity and endothermic nature of the process. The newly synthesized composite attributed to its cost effective and environment friendly nature and ease of synthesis, could be deemed as a potential candidate for the removal of Cd(II) and Pb(II) ions from waste-water.

GRAPHICAL ABSTRACT



INTRODUCTION

Heavy metal pollution is a serious environmental problem of global concern caused by rapid growth in industrialization. They are generally hazardous, non-biodegradable and persistent in nature.¹ They cause serious detrimental effects on biotic as well as abiotic segments of ecosystem including health hazards in human and plants.² These metals include Pb, Cd, Cr, As etc.³ Metal plating, lead acid batteries, printing,

glass and ceramic industries, lead mining, phosphate fertilizers, forest fires, electronics, and automobile emission are the major sources of lead (Pb) pollution.⁴ Pb has been reported with problems like brain and kidney dysfunction, miscarriage, under developed fetus, disruption of nervous system and infertility.⁵ Severe exposure to Pb causes abortion, sterility, neo-natal deaths and stillbirths.⁶ The world health organization (WHO) drinking water standard for Pb is 0.01 mg/L.⁷ Similar to Pb, cadmium (Cd) is

* Corresponding author: atasafi@hotmail.com

another highly toxic pollutant released by industries like metallurgical alloying, photography, electroplating, Cd batteries, pigments, textile print, phosphate fertilizers etc.⁸ Toxicity of Cd causes cancer, bone lesions, hypertension, lung deficiency and Itai-Itai.⁹ Attributed to its highly toxic nature, WHO has crammed its permissible limit in drinking water to 0.02 mg L⁻¹.¹⁰ Due their toxic and detrimental effects on living organisms and environment, removal of Cd and Pb from aqueous media has been a major centre of research for scientists.

Many approaches have been adopted for the removal of heavy metal including chemical precipitation,¹¹ electrochemical treatment,¹² chemical oxidation/reduction,¹³ reverse osmosis,¹⁴ ion exchange,¹⁵ electro dialysis¹⁶ and evaporation.¹⁷ These techniques usually require high maintenance cost and expensive facilities. On the contrary, researchers are always craving a low cost, simplified, effective and environment friendly method as alternative approach. In this regard, adsorption is considered an economical, effective, simple and widely applied method.¹⁸ Rice husk,¹⁹ corncorb,²⁰ tea waste,²¹ bagasse fly ash,²² sawdust (*Pinus halepensis*),²³ meranti tree sawdust,²⁴ coconut shells,²⁵ apricot stone,²⁶ rice husk ash,²⁷ walnut sawdust,²⁸ olive cake²⁹ and pine sawdust (*Pinus sylvestris*)³ have been reported for the removal of Cd and Pb from aqueous solutions. To the best of our knowledge, no reports on the application of poly(acrylic acid-co-acrylamide)/sawdust (PAA-SD) composite for the adsorptive removal of Pb and Cd has been reported so far.

Thus, this study focuses on the synthesis of PAA-SD composite by the combination of *Dalbergia sissoo* (sheesham) sawdust (SD) and poly(acrylic acid-co-acrylamide) for adsorptive removal of Cd(II) and Pb(II) from aqueous solutions. Reaction parameters were optimized and experimental data were applied to kinetic models for better understanding of the reaction pathway. The pristine sawdust and final composite were characterized by X-ray diffraction (XRD), scanning electron microscopy (SEM), Brunauer–Emmett–Teller (BET), energy dispersive X-ray analysis (EDX) and Fourier transformed infra-red (FTIR) spectroscopy.

EXPERIMENTAL

1. Materials

All the reagents were of analytical grade and used without further purification. Monomers acrylic acid (99%), Potassium persulfate (KPS 98%) and acrylamide (98%) were obtained from DAEJUNG reagents chemicals. KPS and Sodium sulphite (95%) anhydrous (by Riedel-deHaën) were used as

initiator and accelerator, respectively. Sodium hydroxide (99%) was provided by Merck. Cross-linker N,N-methylenebisacrylamide (MBA, 98.5%) was provided by UNI-Chem® chemical reagents. Double distilled water was used throughout the experimental work.

2. Sawdust

Dalbergia sissoo SD was obtained from timber shop near Peshawar University, KP, Pakistan. The sample was washed with water to remove surface impurities and dried for 24 h at ambient temperature. The SD sample was put in quartz tube which was then placed in tubular furnace and heated at 170 °C (± 5 °C) for 45 minutes in nitrogen flow rate of 40 mL/minute. This activated sample was washed in a soxhlet extractor at 100 °C with distilled water and dried in oven for five hours at 110 °C. Dried samples were screened from 100 μ m mesh (U.S Standard sieve).

3. Synthesis

of poly(acrylic acid-co-acrylamide) copolymer

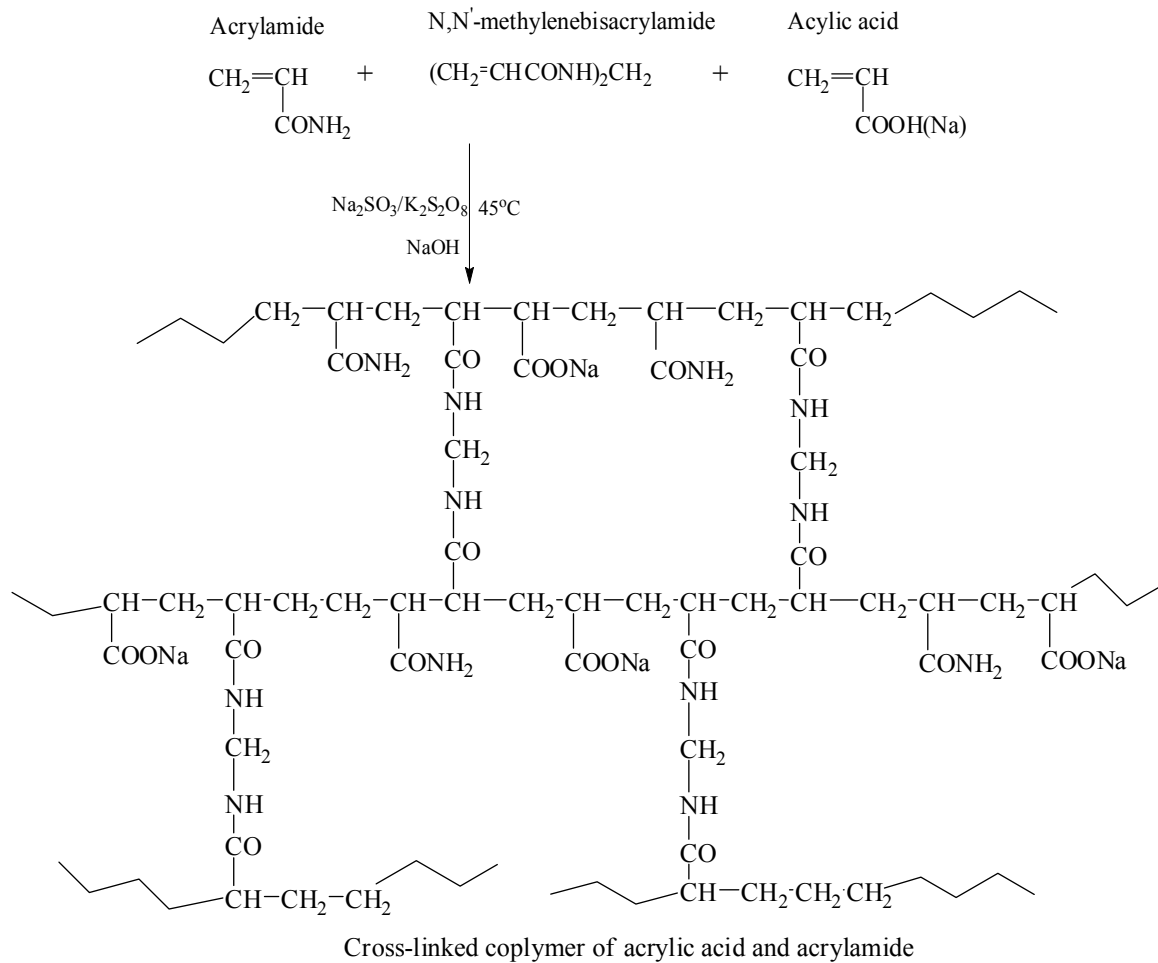
Cross-linked copolymer of acrylic acid (3 mL) and acrylamide (0.2 g) were prepared by solution polymerization method using acrylic acid monomer, acrylamide and N,N-methylenebisacrylamide (MBA, 0.2 g). A redox initiating system, consisting of potassium persulfate and sodium sulphite (0.2 g each) was used as an initiator. The proposed mechanism for the reaction is provided in Scheme 1 below.

4. Synthesis of poly(acrylic acid-co-acrylamide)/Sawdust composite (PAA-SD)

A PAA-SD composite was synthesized by solution polymerization method reported elsewhere.³⁰ Acrylic acid (3 mL) was dissolved in 20 mL distilled water and solution was partially neutralized with sodium hydroxide solution up to 60%. Sawdust (2 g in 70 mL distilled water) was dispersed in partially neutralized acrylic acid and acrylamide (0.2 g in 10 mL distilled water) solutions. No sawdust precipitation was observed. The cross-linker, MBA (0.2 g dissolved in 10 mL distilled water) was added to the mixture of clay solution under N₂ atmosphere. Mixture was placed in three-necked round bottom flask followed by its heating in water bath at 45°C for 15 min with uniform shaking via mechanical stirrer at 250 rpm till complete dissolution of MBA. Initiators (Na₂SO₃ and KPS, 0.2 g of each dissolved in 10 mL distilled water separately) were added to the flask and stirred for 30 min to ensure complete consumption of monomers and composite formation. The rubbery gel was removed from the flask and dried at 80 °C in vacuum oven till solid mass is obtained.

5. Characterization

The FTIR spectra of PAA-SD composite were recorded on FTIR, Model 1760x, Perkin-Elmer Infrared Spectrometer. The structure and crystallinity of the composite was identified using XRD Model JDX-3532 (JEOL, Japan) operating with Cu-K α radiations ($\lambda = 1.5418$ Å) at an angle (2θ) ranging from 0 to 80°, an accelerating voltage of 20-40 kV and an applied current of 2.5-30 mA. Elemental analysis was conducted using EDX analyzer (INCA-200/Oxford instruments, U.K) fixed with SEM (JSM 5910, JEOL Japan). The morphology of PAA-SD composite was examined using SEM (Model JSM-5910 JEOL Japan). Surface area of the composite was determined by N₂ adsorption of method at 77 K applying BET technique surface area analyzer (NOVA 2200e, Quantachrome, USA).



Scheme 1 – Synthesis route and structure of Poly(acrylic acid-co-acrylamide) copolymer.

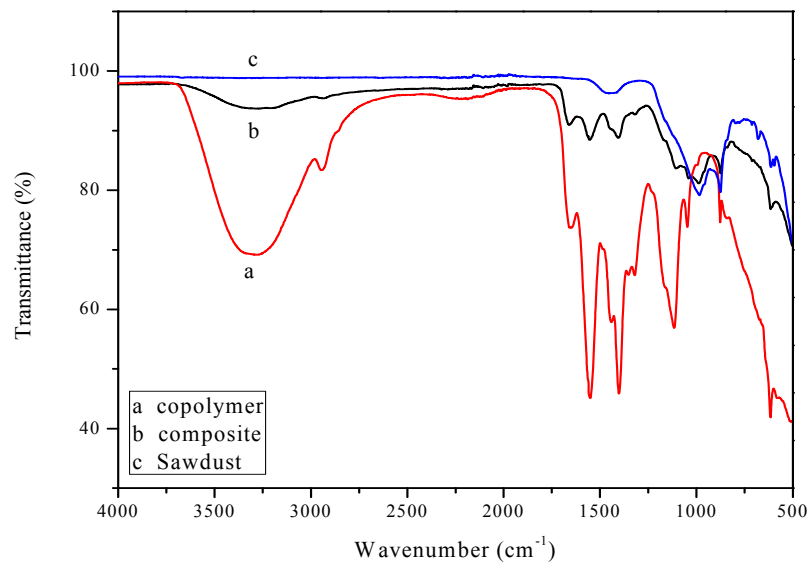


Fig. 1 – FTIR spectra of sawdust, copolymer and composite.

6. Adsorption experiments

Separate aqueous solutions of Cd(II) and Pb(II) ions (100 ppm each) were used to conduct adsorption experiments. In a typical run, 40 mL of adsorbate and 0.3 g of PAA-SD

were taken in a conical flask and shaken in water shaker at 150 rpm and 25 °C for 3 h. After shaking, solutions were filtered through Whatman 125 mm filter paper and analyzed for Cd(II) and Pb(II) ions concentration using Atomic adsorption spectrometer (AAS) by Eq. (1).

$$q = \frac{(C_o - C_e)}{m} \times V \quad (1)$$

where q is the amount of metal ions adsorbed onto the composite (mg g^{-1}), C_o and C_e are the concentration of metal ions in the initial solutions and at equilibrium, respectively (mg mL^{-1}), V is the volume of the aqueous phase (mL), and m is the mass of PAA-SD composite (g).

RESULTS AND DISCUSSION

1. FTIR spectrum of sawdust, copolymer and PAA-SD composite

FTIR spectrum of *Dalbergia sissoo* SD in Fig. 1 shown by (c) suggests its complex chemical nature with a variety of functional groups. The peaks at 1449, 1283, 989, 870, 811, 669, 621 cm^{-1} represent symmetric bending of CH_3 , surface hydroxyl, phenolic group stretching, CO phenolic group stretching, cellulose, CH bending, NH bond and alkyl halide groups of CBr stretching vibration, respectively.³¹ Similarly, FTIR spectrum of poly(acrylic acid-co-acrylamide) copolymer in Fig. 1 shown by (a) shows peaks at 3315, 2960, 2586, 1627 and 1408 cm^{-1} ascribed to NH stretching vibration of acrylamide unit, acrylate unit of CH stretching, OH stretching, stretching of C = O in acrylate unit and CN group, respectively.³² These results confirmed the successful reaction between acrylic acid and acrylamide.³²

The FTIR spectrum of PAA-SD composite is given in Fig.1 shown by (b). The 3273, 2948 cm^{-1} peaks indicate stretching vibration of OH band and stretching vibration of CH, respectively.

Stretching vibration of C = O carboxylic groups are shown by 1760 cm^{-1} and 1260 cm^{-1} while 1558 cm^{-1} is related to C = O bond. Peak at 1395 cm^{-1} is due to OH bending and 1125 cm^{-1} shows CO stretching vibration of acrylic ester groups. The peaks at round 896, 827 and 611 cm^{-1} are due to C–H bending. In the spectra of composite, compared with sawdust and copolymer, some peaks changed in intensity and new peaks appeared which gives the confirmation of reaction between sawdust and copolymer chain.^{33–35}

2. XRD analysis

XRD analysis is a useful tool for intercalation in sawdust investigations. Fig. 2 shows the XRD patterns of SD, copolymer and their composite, respectively. It was observed that PAA-SD composite diffraction peaks were the same as in raw SD at 10.900° is the peak, indicates that the poly(AAc-co-AAm) do not penetrate in the interlayer space efficiently and only covered the surface of SD. It may be due to the large molecular structure of poly(AAc-co-AAm). Similar results are obtained by Huang R *et al.* when HACC used for medication of bentonite, surface of bentonite is covered by the HACC. Moreover, a clear crystallization 32.350° peak is seen in poly(AAc-co-AAm). However, this peak disappeared in PAA-SD composite. Intensity of 10.900° diffraction peak in SD is very weak as compared to composite and suggesting high degree of interaction between poly(AAc-co-AAm) with SD resulting in the successful formation of the composite.^{36,37}

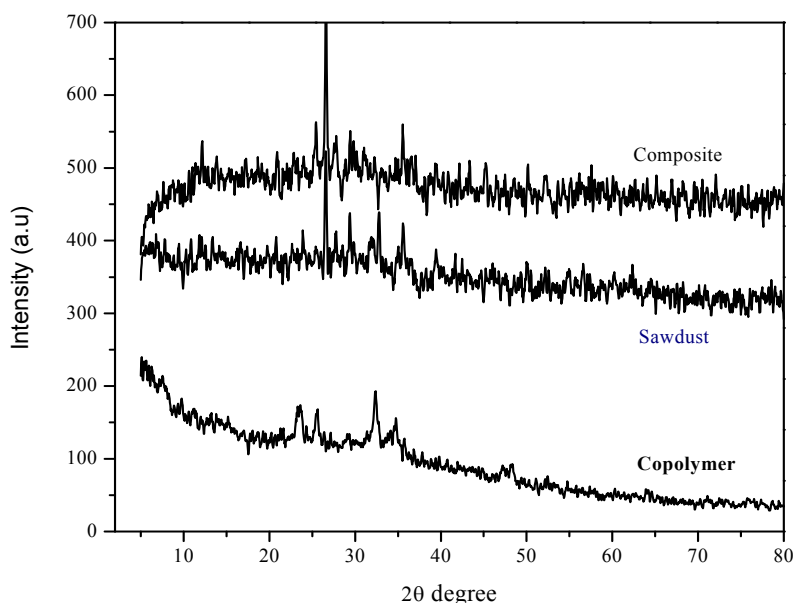


Fig. 2 – XRD spectra of (a) copolymer (b) sawdust and (c) composite.

3. SEM analysis

SEM has been ubiquitously used for characterizing the surface morphology, particle shape, adequate size of pores and porosity of adsorbents. Fig. 3 (a), (b) and (c) show the SEM images of sawdust, copolymer and PAA-SD composite, respectively. The image of sawdust is dark field with rough surface. The surface is porous though are not scattered unevenly in the whole matrix. Due to inorganic elements the surface, flakes as confirmed by the EDX analysis.³⁸ Fig. 3 (c) shows the SEM image of composite which suggests a number of pores in different shapes and size compared with sawdust and copolymer. It is suggested that these pores are the region of adsorption for toxic metals from contaminated water. Roughness of surface indicates the high surface area.

4. Surface area analysis

In any adsorption or surface interaction based process, surface area plays an important role and greater surface provide higher chances of adsorbent-heavy metal ion interaction resulting in higher adsorption capacity and vice versa.³⁹ The BET surface area of the composite was determined by N₂ adsorption method⁴⁰ and was found to be 32.316 m²/g.

5. EDX analysis

EDX study of sawdust, copolymer and PAA-SD composite was conducted to test their elemental composition. The atomic % and weight % of different elements were determined and shown in Fig. 4(a), (b) and (c), which indicated that composite has the highest percentage of oxygen (40.50%) followed by carbon (39.94%) and nitrogen (5.24%).

4. Adsorption studies

4.1. Effect of initial concentration

Effect of initial concentration of Cd(II) ions on composite is shown in Fig. 5. With increase in initial concentration from 20-250 ppm, using 0.3 g/40 mL adsorbent dose, the adsorption efficiency increases. At higher initial concentration, adsorption is fast owing to high availability of active sites on surface of composite then increases slowly and attains a constant value. Further increase in

concentration has no prominent effect on adsorption owing to the saturation of active sites on composite with heavy metals ions. Maximum amount of Cd(II) ions is adsorbed at a concentration of 200 mg L⁻¹. Similar trend in adsorption results was obtained for Pb(II) ions on PAA-SD composite.

4.2. Effect of contact time

The effect of contact time on the adsorption of Cd(II) and Pb(II) over composite was studied at an initial metal ion concentration of 200 ppm, 0.3 g adsorbent and 40 mL of ion solution. From Fig. 6 it is clear that adsorption rate is very fast initially (first 20 min) and keeps on increasing slowly till 60 min before attaining equilibrium. The initial high adsorption rate is due to the abundance of free adsorption sites, which become saturated with the passage of time and results in decreased adsorption rate. From Fig. 6, a contact time of 60 min was chosen for onward experiments.

4.3. Effect of pH

The effect of pH on the adsorption of Cd(II) and Pb(II) on PAA-SD composite was studied and the results are compiled in Fig. 7. The adsorption of Cd(II) increases with increasing pH and maximum adsorption was observed at pH 5. With further increase in pH, adsorption decreases. A similar trend for the adsorption of Pb(II) was also observed by varying pH from 2 to 9. The maximum adsorption was observed at pH 6 but adsorption decreases with further increase of pH. At lower pH, lower adsorption was due to competitive adsorption between H⁺ ions and metal ions towards active sites. Moreover, the positive charges is increased on the surface of composite which hinder further adsorption of positively charged metal ions due to electrostatic repulsion. Thus pH 6 was chosen as optimum pH for both the metal ions, which consistent with some reported literature for Cd(II) and Pb(II) adsorption.⁴¹

4.4. Effect of temperature

Temperature is an important factor that greatly affects the adsorption process. Effect of temperature on the adsorption of the two metals was studied in a range of 25-45 °C as shown in Fig. 8. The rate of adsorption of Cd(II) and Pb(II) increased by increasing temperature from 25 to 45 °C, indicating the endothermic nature of adsorption process. This may be due to fast molecular movements and activation of Cd(II) and Pb(II) towards the active sites of adsorbent.

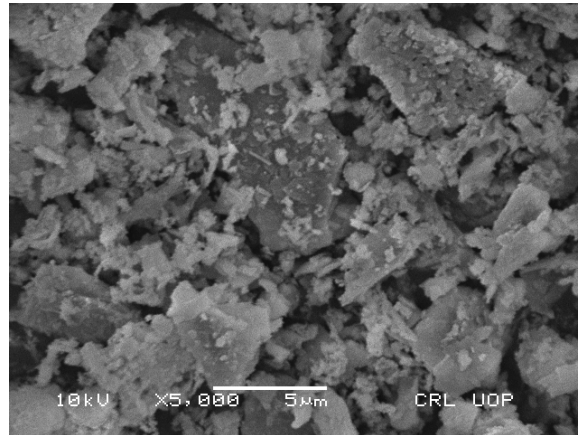


Fig. 3(a) – SEM image of sawdust.

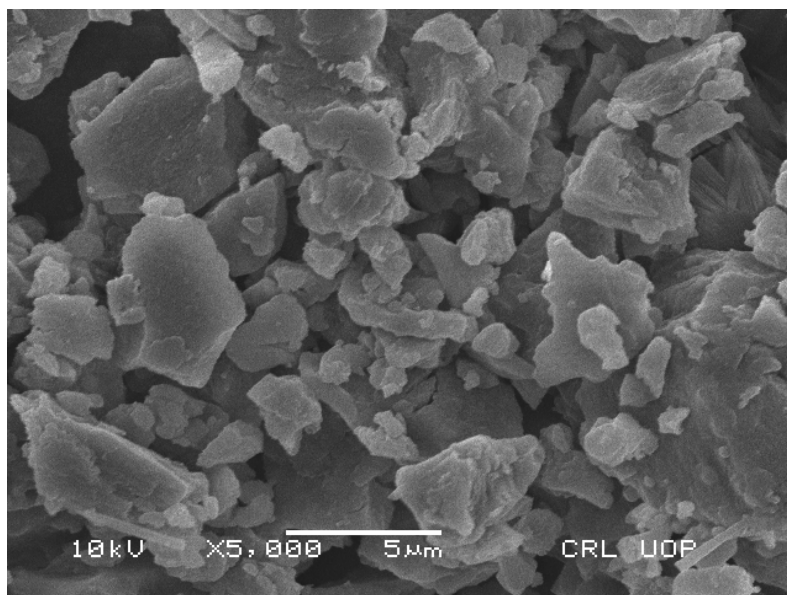


Fig. 3(b) – SEM image of copolymer.

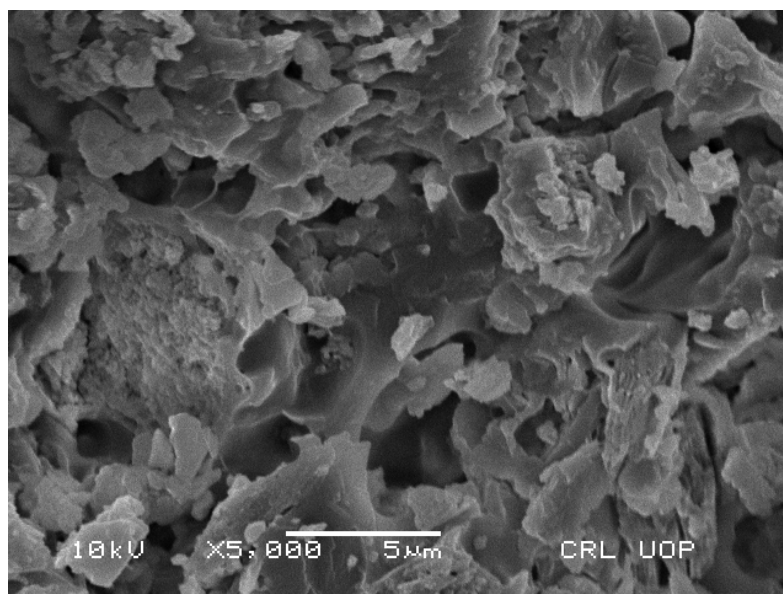


Fig. 3(c) – SEM image of PAA-SD composite.

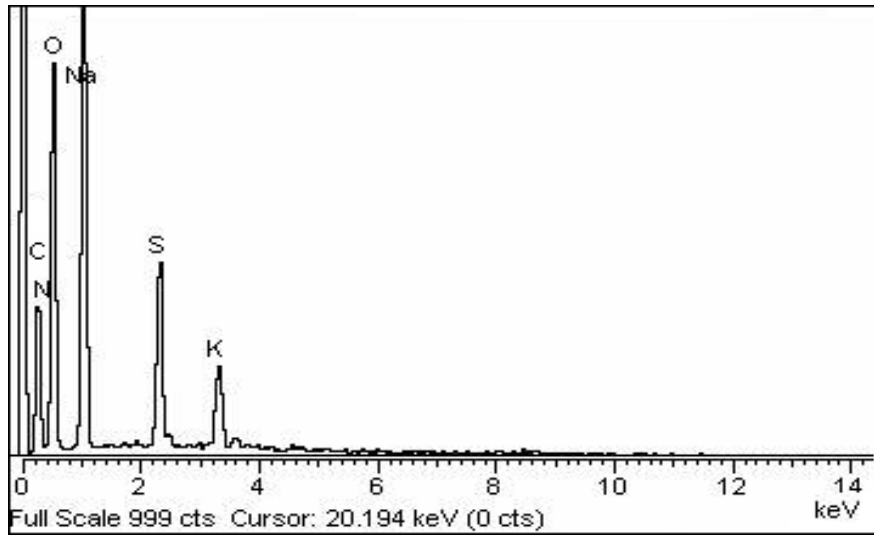


Fig. 4(a) – EDX spectrum of PAA copolymer.

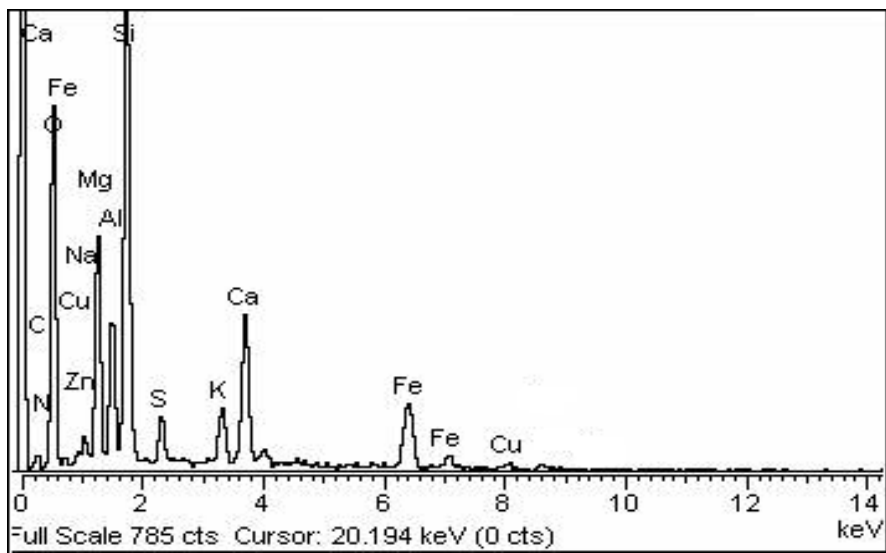
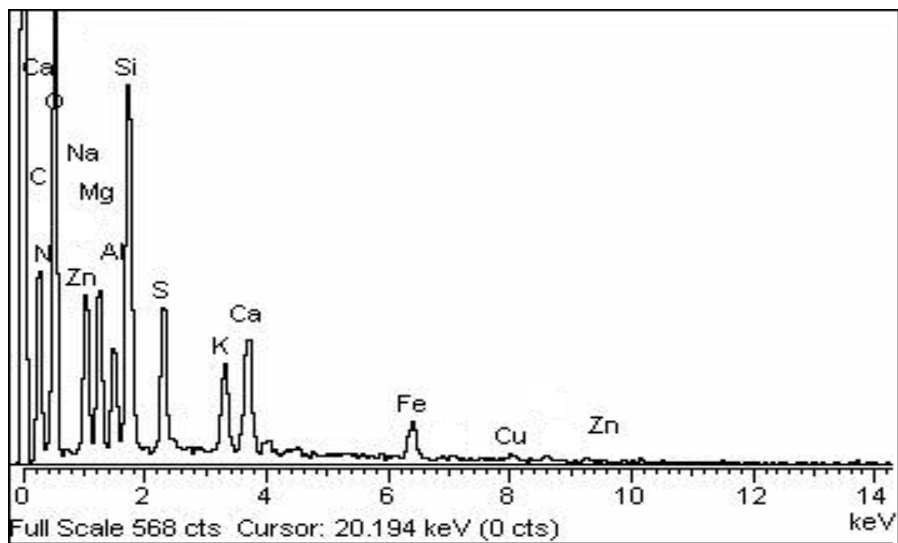
Fig. 4(b) – EDX spectrum of *Dalbergia sissoo* SD.

Fig. 4(c) – EDX spectrum of PAA-SD composite.

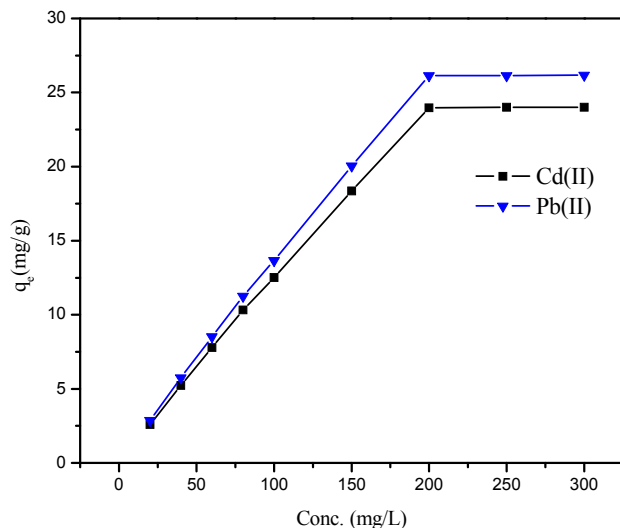


Fig. 5 – Effect of initial metal ion concentration on PAA-SD composite at 25 °C, 0.3 g of adsorbent and 40 mL of sample solution.

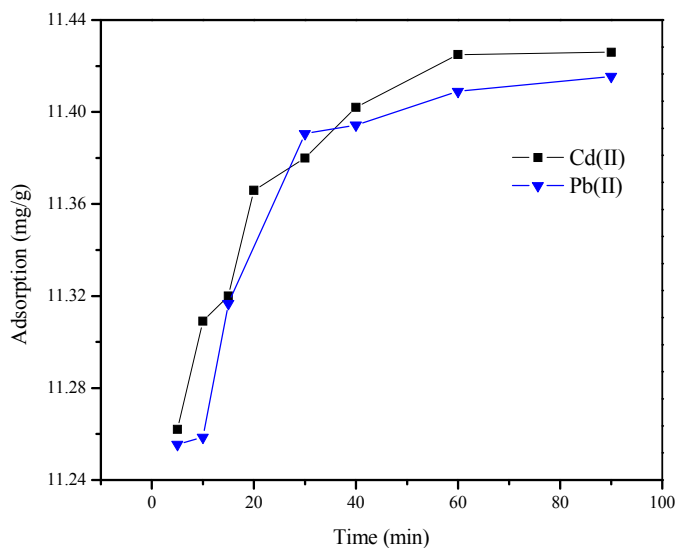


Fig. 6 – Effect of contact time on the adsorption of Cd(II) and Pb(II) ions at 25 °C, 0.3 g of adsorbent and 40 mL of 200 ppm sample solution.

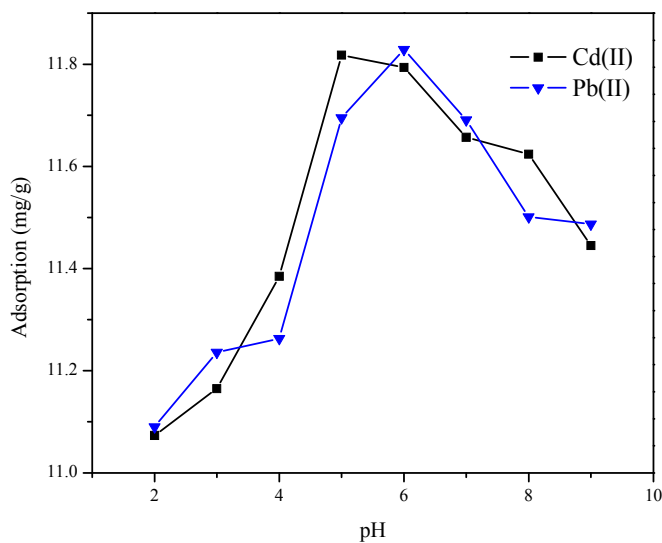


Fig. 7 – Effect of pH on adsorption of Cd(II) and Pb(II) ions on PAA-SD composite at 25 °C, 0.3 g of adsorbent, 60 min time, and 40 mL of 200 ppm sample solution.

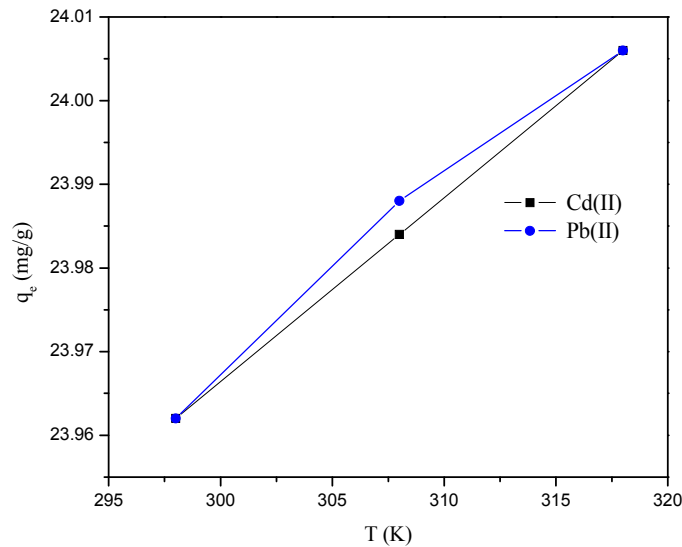


Fig. 8 – Effect of temperature on adsorption of Cd(II) and Pb(II) ions on PAA-SD composite.

5. Adsorption kinetics

The adsorption kinetics is an important parameter with respect which can better describe the nature and path of adsorption process using some well-established mathematical equations to determine adsorption rate. In order to study the adsorption process of Cd(II) and Pb(II) ions on composite, pseudo first order and pseudo second order models were applied to experimental data.

a. Pseudo first order

The pseudo first order shown by Eq. (2) given by Lagergren was used to analyze the experimental data.⁴²

$$\log(q_e - q_t) = -\frac{k_1 t}{2.303} + \log q_e \quad (2)$$

where q_e (mg g^{-1}) is the amount of metal ion adsorbed at equilibrium, q_t (mg g^{-1}) is the amount of metal ions adsorbed at time t and k_1 (min^{-1}) is the rate constant. The values of k_1 and q_e were calculated from the slope and intercept of straight line plot of $\log(q_e - q_t)$ versus t (Fig. 9), respectively and were reported in Table 1. Greater discrepancies were observed between q_e values determined from the model and experimental. This suggested that the current adsorption process of Cd(II) and Pb(II) did not follow pseudo first order kinetics.

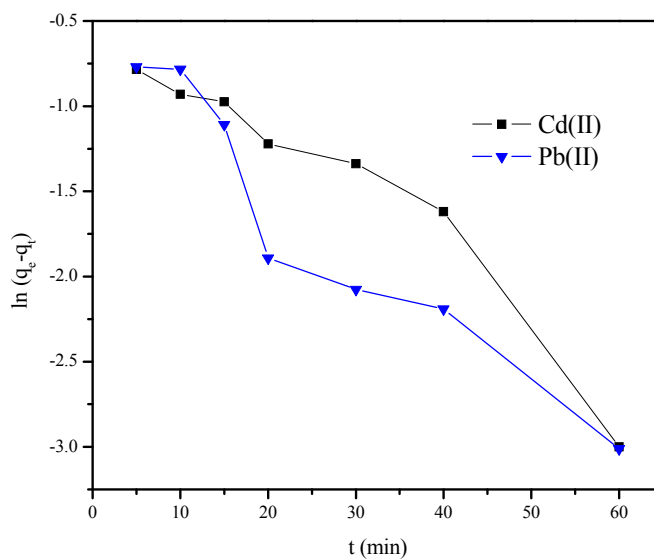


Fig. 9 – Plot of pseudo first order kinetics for Cd(II) and Pb(II) ions adsorption on PAA-SD composite.

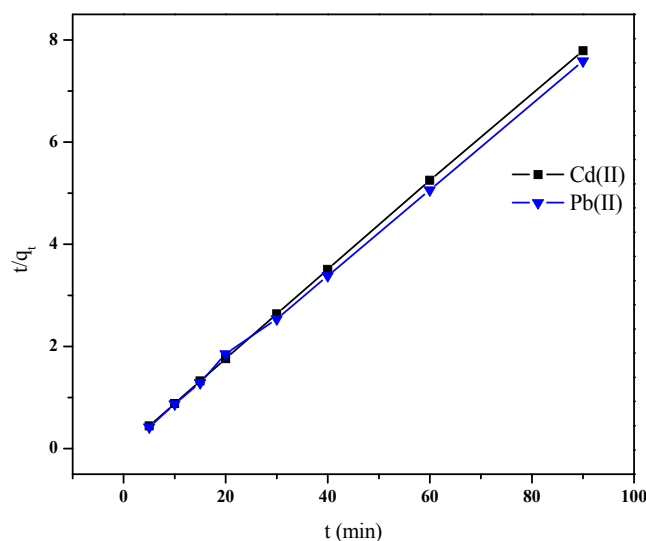


Fig. 10 – Plot of pseudo second order kinetics for Cd(II) and Pb(II) ions adsorption on PAA-SD composite.

b. Pseudo second order

Pseudo second order kinetic model suggested by McKay and Ho was also used to explore the metal ions adsorption data using equation (3).⁴³

$$\frac{t}{q_t} = \frac{1}{k_2 q_e^2} + \frac{1}{q_e} t \quad (3)$$

where k_2 ($\text{g mg}^{-1} \text{min}^{-1}$) is the rate constant of pseudo second order kinetics and q_e and q_t are the same as those mentioned in Eq. (1). The values of k_2 and q_e were calculated from the slope and intercept of straight line plot of t/q_t versus t (Fig. 10), respectively and reported in Table 1. The regression coefficient (R^2) values for Cd(II) and Pb(II) were 1.0 and 0.999, which showed the well fitting of experimental data with pseudo second order kinetics. Moreover, the calculated values of q_e agree significantly with the experimental q_e values suggest that the process followed pseudo second order kinetics.

6. Adsorption isotherms

Adsorption isotherms are very important to design the nature of adsorption process. In the current experimental set up, two well-known isothermal models *i.e.* Freundlich and Langmuir isotherms were applied to experimental data.⁴⁴

a. Langmuir isotherm

The Langmuir isotherm suggests that adsorption of metal ions from aqueous solutions occurs on homogenous surface by monolayer coverage with interaction among the adsorbed

molecules. The linear form of Langmuir model is given by Eq. (4)⁴⁵ as:

$$\frac{C_e}{q_e} = \frac{1}{K_L q_m} + \frac{1}{q_m} \times C_e \quad (4)$$

where C_e is the equilibrium concentration of metal ions (mg L^{-1}), q_e is the amount (mg g^{-1}) of metal ions adsorbed, q_m and K_L are Langmuir constants which indicate the adsorption capacity (mg g^{-1}) and energy of adsorption (L mg^{-1}), respectively. The plots of Langmuir isotherms for Cd(II) and Pb(II) ions are given in Fig. 11. The value of q_m and K_L were calculated from the slope and intercept of linear plot of C_e/q_e vs C_e and represented in Table 2, which suggested an increase in their values with increasing temperature. The maximum adsorption capacities for Cd(II) and Pb(II) ions over PAA-SD composite at 25 °C were 28.571 mgg^{-1} and 32.25 mgg^{-1} respectively.

Weber and Chackravorti 1974, expressed the Langmuir isotherm in terms of a dimensionless constant called equilibrium parameter or separation factor (R_L), which is defined by Eq. (5)⁴⁶.

$$R_L = \frac{1}{1 + bC_i} \quad (5)$$

where K_L is the Langmuir constant and C_i is the initial concentration of metal ion. Literature revealed that if R_L value is less than 1 and greater than zero ($0 < R_L < 1$), adsorption is favorable while if $1 < R_L$ adsorption is unfavorable. If R_L value is equal to zero and 1 suggests the irreversible and reversible nature of the adsorption process respectively.⁴⁷ The values of R_L for adsorption of Cd(II) at 25, 35 and 45 °C were

found to be 0.217, 0.183 and 0.147, respectively while for Pb(II) under similar conditions were 0.208, 0.196 and 0.190, respectively. These results suggested the highly favorable nature of the selected metals ions over PAA-SD composite under the specified experimental conditions.

a. Freundlich isotherm

Freundlich isotherm is an empirical equation that describes the adsorption on heterogeneous adsorbents with interaction among adsorbed molecules. Freundlich adsorption isotherm can be defined by Eq. (6)⁴⁸ in linear form:

$$\ln q_e = \ln K_F + \frac{1}{n} \ln C_e \quad (6)$$

where K_F ($L g^{-1}$) and $1/n$ are Freundlich constants, indicating the adsorption capacity and adsorption intensity, respectively. The plots of Freundlich isotherms for Cd(II) and Pb(II) are given in Fig. 12. Both $1/n$ and K_F were calculated from the slope and intercept of plot of $\ln q_e$ vs $\ln C_e$ and represented in Table 2. Since the values of $1/n$ is lower than 1 showing favorable adsorption scenario. It was found that the adsorption of metal ions on PAA-SD composite fit well with

Freundlich isotherm ($R^2 = 0.956, 0.971$) as compared to the Langmuir isotherm ($R^2 = 0.952, 0.922$) under identical experimental concentration. Using least square method, the isotherm data were calculated and the concerned correlation coefficients are given in Table 2. Reaction parameters were optimized and experimental data were evaluated using kinetic models for better understanding of the reaction pathway.

7. Activity comparison of PAA-SD composite with reported adsorbents

Table 3 shows the comparison of maximum adsorption capacities of Cd(II) and Pb(II) ions on PAA-SD composite with earlier reported adsorbents. The results indicate that the maximum adsorption capacities of metal ions on PAA-SD composite was higher than those reported in literature. These superior data in terms of adsorption capacity and cost effective nature of PAA-SD composite suggest that this novel composite has high potential for practical application on industrial level involving wastewater treatment.

Table 1

Kinetic constants for Cd(II) and Pb(II) ions adsorption on PAA-SD composite

Metal ion	Pseudo first order parameters			Pseudo second order parameters		
	q_e ($mg g^{-1}$)	K_1 (min^{-1})	R^2	q_e ($mg g^{-1}$)	K_2 ($g mg^{-1} min^{-1}$)	R^2
Cd(II)	2.779	0.0852	0.915	11.494	1.081	1.0
Pb(II)	1.183	0.0575	0.918	11.363	0.0944	0.999

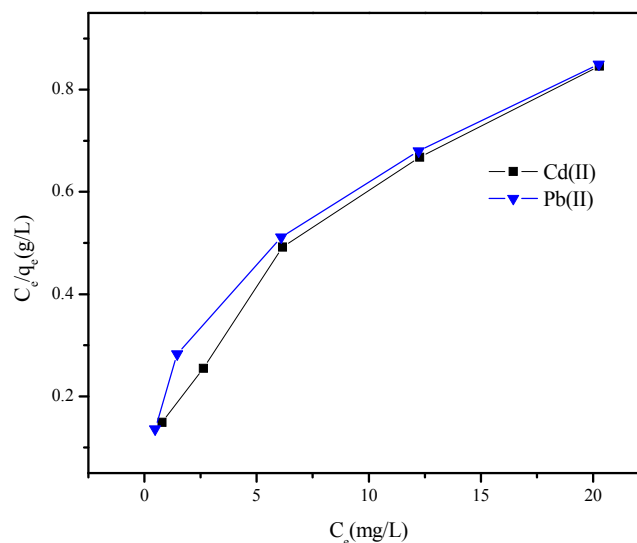


Fig. 11 – Plot of Langmuir isotherms for Cd(II) and Pb(II) adsorption on PAA-SD composite at 25 °C.

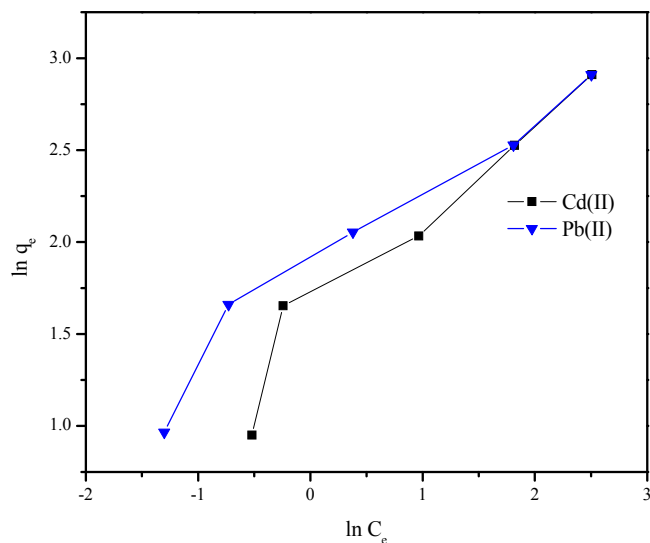


Fig. 12 – Plot of Freundlich isotherms for adsorption of Cd(II) and Pb(II) on PAA-SD composite at 25 °C.

Table 2

Comparison of isotherm constants for Cd(II) and Pb(II) ions adsorption on PAA-SD composite at different temperatures

Metal ion	Temperature (K)	Langmuir's constants			Freundlich's constants		
		q_{\max} (mgg ⁻¹)	$K_L 10^{-2}$ (L/mg)	R^2	$1/n$ (mg/g)	K_F (mg/L)	R^2
Cd(II)	298	28.571	17.98	0.952	0.562	4.486	0.956
	308	29.411	22.22	0.951	0.511	5.338	0.947
	318	30.300	29.00	0.946	0.458	6.104	0.960
Pb(II)	298	32.25	19.00	0.922	0.468	6.043	0.971
	308	33.33	20.40	0.918	0.343	6.952	0.978
	318	34.48	21.30	0.915	0.448	7.249	0.928

Table 3

Comparison of adsorption capacity of PAA-SD composite with reported adsorbents

Adsorbent	Modifying agent (s)	Heavy metal	q_{\max} (mg g ⁻¹)	Reference
Rice husk	Sodium hydroxide	Cd(II)	20.24	19
Cornorb	Nitric acid	Cd(II)	19.3	20
Rice husk ash	Without any pretreatment	Cd(II)	3.0392	49

Table 3 (continued)

Sawdust of deciduous trees	No treatment	Cd(II)	3.5	50
Bamboo charcoal	Washed with water	Cd(II)	12.08	51
Sawdust	Washed with deionized water	Pb(II)	21.05	52
Modified peanut husk	Formalin	Pb(II)	29.14	
Meranti tree sawdust	Formaldehyde	Pb(II)	31.95	53
Empty fruit bunch fiber	NaOH	Pb(II)	20.00	54
Apricot stone	Sulphuric acid	Pb(II)	21.38	26
PAA-SD	Composite	Cd(II)	28.57	Present work
		Pb(II)	32.25	

8. Adsorption thermodynamics

The values of free energy change (ΔG°) for adsorption process were calculated, using the Eq. (7).⁵⁵

$$\Delta G^\circ = -RT \ln K \quad (7)$$

Where R ($8.314 \text{ J mol}^{-1} \text{ K}^{-1}$) is universal gas constant and T (K) is the absolute temperature. The values of thermodynamic parameters are given in Table 4. The negative value of ΔG° shows the spontaneous and feasible nature of adsorption. The values of ΔH° and entropy change ΔS° can be determined using Van't Hoff equation as Eq. (8).⁵⁶

$$\ln K = \frac{\Delta S^\circ}{R} - \frac{\Delta H^\circ}{RT} \quad (8)$$

$$\Delta G^\circ = \Delta H^\circ - T\Delta S^\circ \quad (9)$$

The ΔS° and ΔH° were calculated from the slope of and intercept of $\ln K$ vs $1/T$ given in Fig. 13. The positive values of ΔH° confirmed the endothermic nature of adsorption, while the positive values of ΔS° show the high randomness on active sites during adsorption. The activation energy for adsorption of Cd(II) and Pb(II) ions were calculated using Arrhenius equation as Eq. (10).

$$\ln K = \ln A - \frac{E_a}{RT} \quad (10)$$

The activation energy was calculated from the slope of plot of $\ln K$ vs $1/T$ as given in Fig. 13 and

was found to be $12.148 \text{ kJ mol}^{-1}$ for Cd(II) and $7.165 \text{ kJ mol}^{-1}$ for Pb(II). These results confirmed that the adsorption of metal ions on PAA-SD composite was physical. The physical adsorption process has energy in the range of $5\text{-}40 \text{ kJ mol}^{-1}$ while chemical adsorption process has $40\text{-}800 \text{ kJ mol}^{-1}$ energy.⁵⁷

CONCLUSIONS

A novel PAA-SD composite was synthesized and used as a cost effective adsorbent for the removal of Cd(II) and Pb(II) from aqueous solutions. Adsorption was found dependent on temperature, contact time, pH and initial metal ion concentration. The adsorption kinetics followed pseudo second order kinetic model. Adsorption isotherms were applied to the experimental data which fitted well with Langmuir and Freundlich isotherms. The maximum adsorption capacities, q_m (from Langmuir model) Cd(II) and Pb(II) ions at 25°C , were 28.57 mg g^{-1} and 32.25 mg g^{-1} respectively. The activation energy values $12.148 \text{ kJ mol}^{-1}$ and $7.165 \text{ kJ mol}^{-1}$ for Cd(II) and Pb(II) suggested physical adsorption. The thermodynamic parameters showed the exothermic, feasibility and spontaneous nature of the adsorption. The PAA-SD composite showed superior adsorption capacities for Cd(II) and Pb(II) than some adsorbent reported in literature. The cost effective nature and high adsorption capacity of PAA-SD for Cd(II) and Pb(II) rank it as a potential contender for waste-water treatments on industrial level.

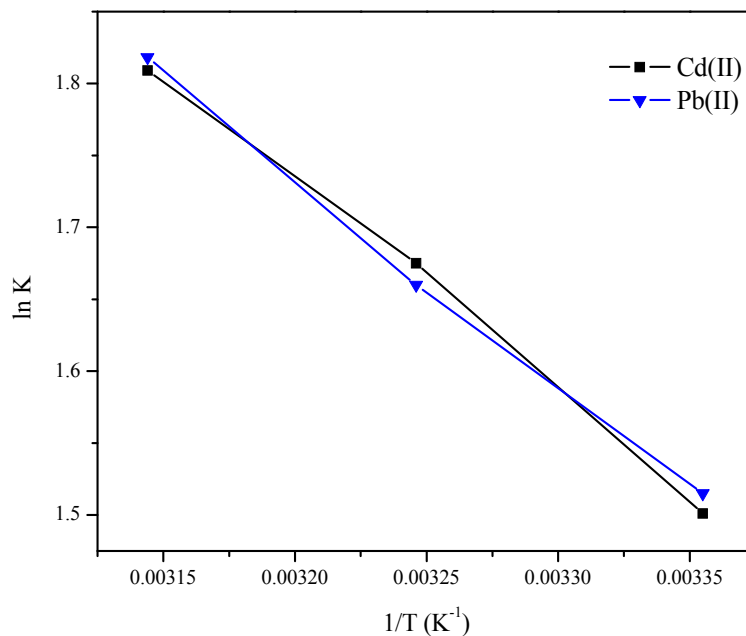


Fig. 13 – Plot of Van't Hoff equation for Cd(II) and Pb(II) ions adsorption on PAA-SD composite.

Table 4

Thermodynamics parameters for Cd(II) and Pb(II) ions adsorption on PAA-SD composite at different temperatures

Metal ion	Temperature (K)	K_F (L/g)	ΔH° (kJmol ⁻¹)	ΔS° (kJmol ⁻¹ K ⁻¹)	ΔG° (kJmol ⁻¹)
Cd(II)	298	4.486	12.146	0.0532	- 3.718
	308	5.338	---	0.0533	- 4.289
	318	6.104	---	0.0532	- 4.782
Pb(II)	298	6.043	7.165	0.0390	- 4.457
	308	6.952	---	0.0389	- 4.829
	318	7.249	---	0.0390	- 5.237

REFERENCES

1. M. Hashim, S. Mukhopadhyay, J. N. Sahu and B. Sengupta, *J. Environ. Manage.*, **2011**, *92*, 2355.
2. A. Demirbas, *J. Hazard. Mater.*, **2004**, *109*, 221.
3. V. C. Taty-Costodes, H. Fauduet, C. Porte and A. Delacroix, *J. Hazard. Mater.*, **2003**, *105*, 121.
4. V. K. Gupta, S. Agarwal and T. A. Saleh, *J. Hazard. Mater.*, **2011**, *185*, 17.
5. B. Yu, Y. Zhang, A. Shukla, S. S. Shukla and K. L. Dorris, *J. Hazard. Mater.*, **2001**, *84*, 83.
6. S.-H. Kim, H. Song, G. M. Nisola, J. Ahn, M. M. Galera, C. Hee Lee and W.-J. Chung, *J. Ind. Eng. Chem.*, **2006**, *12*, 469.

7. H. R. Tashauoei, S. Hashemi, R. Ardani, Z. Yavari and M. Asadi-Ghahhari, *J. Saf. Environ. Health Res.*, **2016**, *1*, 11.
8. A. Pérez-Marín, V. M. Zapata, J. Ortuno, M. Aguilar, J. Sáez and M. Lloréns, *J. Hazard. Mater.*, **2007**, *139*, 122.
9. B. Benguella and H. Benaissa, *Water Res.*, **2002**, *36*, 2463.
10. O. Yavuz, R. Guzel, F. Aydin, I. Tegin and R. Ziyadanogullari, *Pol. J. Environ. Stud.*, **2007**, *16*, 467.
11. S. N. do Carmo Ramos, A. L. P. Xavier, F. S. Teodoro, L. F. Gil and L. V. A. Gurgel, *Ind. Crops. Prod.*, **2016**, *79*, 116.
12. A. M. Mahmoud, F. A. Ibrahim, S. A. Shaban and N. A. Youssef, *Egypt. J. Pet.*, **2015**, *24*, 27.
13. T. Sreeprasad, S. M. Maliyekkal, K. Lisha and T. Pradeep, *J. Hazard. Mater.*, **2011**, *186*, 921.
14. H. Ozaki, K. Sharma and W. Saktaywin, *Desalination*, **2002**, *144*, 287.
15. A. Dabrowski, Z. Hubicki, P. Podkościelny and E. Robens, *Chemosphere*, **2004**, *56*, 91.
16. S. Ricordel, S. Taha, I. Cisse and G. Dorange, *Sep. Purif. Technol.*, **2001**, *24*, 389.
17. B. Alyüz and S. Veli, *J. Hazard. Mater.*, **2009**, *167*, 482.
18. C. Xiong, L. Pi, X. Chen, L. Yang, C. Ma and X. Zheng, *Carbohydr. Polym.*, **2013**, *98*, 1222.
19. U. Kumar and M. Bandyopadhyay, *Bioresour. Technol.*, **2006**, *97*, 104.
20. R. Leyva-Ramos, L. Bernal-Jacome and I. Acosta-Rodriguez, *Sep. Purif. Technol.*, **2005**, *45*, 41.
21. S. Cay, A. Uyanık and A. Özaşık, *Sep. Purif. Technol.*, **2004**, *38*, 273.
22. V. C. Srivastava, I. D. Mall and I. M. Mishra, *Chem. Eng. J.*, **2006**, *117*, 79.
23. L. Semerjian, *J. Hazard. Mater.* **2010**, *173*, 236.
24. A. Ahmad, M. Rafatullah, O. Sulaiman, M. H. Ibrahim, Y. Y. Chii and B. M. Siddique, *Desalination*, **2009**, *247*, 636.
25. M. Sekar, V. Sakthi and S. Rengaraj, *J. Colloid Interface Sci.*, **2004**, *279*, 307.
26. L. Mouni, D. Merabet, A. Bouzaza and L. Belkhiri, *Desalination*, **2011**, *276*, 148.
27. Q. Feng, Q. Lin, F. Gong, S. Sugita and M. Shoya, *J. Colloid Interface Sci.*, **2004**, *278*, 1.
28. Y. Bulut and Z. Tez, *Fresen. Environ. Bull. J.*, **2003**, *12*, 1499.
29. S. Doyurum and A. Celik, *J. Hazard. Mater.*, **2006**, *138*, 22.
30. Y. Bulut, G. Akçay, D. Elma and I. E. Serhatlı, *J. Hazard. Mater.*, **2009**, *171*, 717.
31. B. Nagy, A. Maicaneanu, C. Indolean, S. Burca, L. Silaghi-Dumitrescu and C. Majdik, *Acta. Chim. Slov.*, **2013**, *60*, 263.
32. R. Liang and M. Liu, *J. Appl. Polym. Sci.*, **2007**, *106*, 3007.
33. M. A. Wahab, S. Jellali and N. Jedidi, *Bioresour. Technol.*, **2010**, *101*, 5070.
34. M. S. Rahman and M. R. Islam, *Chem. Eng. J.*, **2009**, *149*, 273.
35. J. Singh, N. Mishra, S. Banerjee and Y. C. Sharma, *BioResources*, **2011**, *6*, 2732.
36. R. Huang, B. Wang, B. Yang, D. Zheng and Z. Zhang, *Desalination*, **2011**, *280*, 297.
37. C. Minakshi and S. Arya, *Int. J. Adv. Res. Sci. Technol.*, **2014**, *3*, 99.
38. M. Shakirullah, I. Ahmad and S. Shah, *J. Chin. Chem. Soc.*, **2006**, *53*, 1045.
39. Y. Muhammad, Y. Lu, C. Shen and C. Li, *Energy Convers. Manage.*, **2011**, *52*, 1364.
40. Y. Muhammad, A. Shoukat, A. U. Rahman, H. U. Rashid and W. Ahmad, *Chin. J. Chem. Eng.*, **2018**, *26*, 593.
41. D. Sud, G. Mahajan and M. P. Kaur, *Bioresour. Technol.*, **2008**, *99*, 6017.
42. N. K. Amin, *J. Hazard. Mater.*, **2009**, *165*, 52.
43. M. R. Moghadam, N. Nasirizadeh, Z. Dashti and E. Babanezhad, *Int. J. Ind. Chem.*, **2013**, *4*, 19.
44. B. H. Hameed, D. K. Mahmoud and A. L. Ahmad, *J. Hazard. Mater.*, **2008**, *158*, 65.
45. C. Fan, K. Li, J. Li, D. Ying, Y. Wang and J. Jia, *J. Hazard. Mater.*, **2017**, *326*, 211.
46. Y. Sharma, U. S. Upadhyay and F. Gode, *J. Appl. Sci. Environ. Sanit.*, **2009**, *4*, 21.
47. M. Rauf, S. Bukallah, F. Hamour and A. Nasir, *Chem. Eng. J.*, **2008**, *137*, 238.
48. N. Wang, R. Jin, A. Omer and X. OuYang, *Int. J. Biol. Macromol.*, **2017**, *102*, 232.
49. V. C. Srivastava, I. D. Mall and I. M. Mishra, *Colloids Surf. A. Physicochem. Eng. Asp.*, **2008**, *312*, 172.
50. D. Božić, V. Stanković, M. Gorgievski, G. Bogdanović and R. Kovačević, *J. Hazard. Mater.*, **2009**, *171*, 684.
51. F. Y. Wang, H. Wang and J. W. Ma, *J. Hazard. Mater.* **2010**, *177*, 300.
52. Q. Li, J. Zhai, W. Zhang, M. Wang and J. Zhou, *J. Hazard. Mater.*, **2007**, *141*, 163.
53. A. Ahmad, M. Rafatullah, O. Sulaiman, M. H. Ibrahim, Y. Y. Chii and B. M. Siddique, *Desalination*, **2009**, *247*, 636.
54. M. M. Ibrahim, W. W. Ngah, M. Norliyana, W. W. Daud, M. Rafatullah, O. Sulaiman and R. Hashim, *J. Hazard. Mater.*, **2010**, *182*, 377.
55. C. Lei, X. Zhu, B. Zhu, C. Jiang, Y. Le and J. Yu, *J. Hazard. Mater.*, **2017**, *321*, 801.
56. A. Nashine and A. Tembhurkar, *J. Environ. Chem. Eng.*, **2016**, *4*, 3267.
57. S. Chakravarty, A. Mohanty, T. N. Sudha, A. Upadhyay, J. Konar, J. Sircar, A. Madhukar and K. Gupta, *J. Hazard. Mater.*, **2010**, *173*, 502.

